A Novel Compressed Sensing Based Track before Detect Algorithm for Tracking Multiple Targets

Liu Jing
School of Electronics
and Information Engineering,
Xi'an Jiaotong University,
Xi'an, P.R.China.
Email: elelj20080730@mail.xjtu.edu.cn

Han ChongZhao
School of Electronics
and Information Engineering,
Xi'an Jiaotong University,
Xi'an, P.R.China.
Email: czhan@mail.xjtu.edu.cn

Han Feng
China Huayin Ordnance Test Center
Xi'an, P.R.China.
Email: hf-2105@163.com

***Abstract*—A novel compressed sensing based track-before-detect (TBD) algorithm is presented in this paper, which is named as CS-TBD algorithm. The proposed CS-TBD algorithm reconstructs the whole radar scenario (direction of arrival (DOA)-Doppler plane) for each range gate at consecutive scans using an improved StOMP algorithm, resulting in a three-dimensional range-DOA-Doppler space. The proposed algorithm then performs temporal tracking in the newly built three-dimensional range-DOA-Doppler space, based on the information from multiple illuminations during each scan, as well as among consecutive scans. In the proposed CS-TBD algorithm, the improved StOMP algorithm together with the temporal tracking, can effectively distinguish true targets from false targets and clutter based on information from multiple illuminations.**

I. INTRODUCTION

Track before detect (TBD) based approaches declare the presence of targets and their corresponding tracks through jointly processing several consecutive scans based on the targets' kinematics. A TBD algorithm can improve track accuracy and follow low signal-to-noise ratio (SNR) targets at the price of an increase of the computational complexity.

In recent years, the TBD algorithm has been applied in radar systems [1], [2], [3]. In [1], the continuous-time continuous-amplitude signal is discretized to reflect the sectorization of the coverage area and the range gating operation, and a generalized likelihood ratio test (GLRT) is applied using a Viterbi-like tracking algorithm. In [2], the authors propose a series of TBD strategies for space-time adaptive processing (STAP) radars. Detectors for two different scenarios (equivalent covariance matrices and inequivalent covariance matrices) are derived based on a GLRT and ad hoc procedures. In [3], a number of new algorithms are proposed for adaptive detection and tracking based on spatial-time data. The possible spillover of target energy to adjacent range cells is taken into account in the design stage. In summary, the main problem with TBD techniques is that the measurements depend on the target state in a highly nonlinear way. A possible means to solve the nonlinear filtering problem is to use particle filtering [4]. An alternative is to discretize the target state space [5], [6].

A novel CS-TBD algorithm is proposed in this work. The CS-TBD algorithm was developed and presented in our previous work [7]. The proposed algorithm is different from existing TBD algorithms which adopt hypothesis testing using the radar measurements. The proposed CS-TBD algorithm reconstructs the whole radar scenario (direction of arrival (DOA)-Doppler plane) for each range gate at consecutive scans using an improved StOMP (Stagewise OMP, [8]), resulting in a three-dimensional range-DOA-Doppler space. It then performs temporal tracking in the newly built three-dimensional range-DOA-Doppler space, based on the information from multiple illuminations during each scan, as well as among consecutive scans. The proposed algorithm avoids the nonlinear problem since it tracks and detects multiple targets in the reconstructed range-DOA-Doppler space. In the proposed CS-TBD algorithm, the improved StOMP algorithm together with the temporal tracking, can effectively distinguish true targets from false targets and clutter based on information from multiple illuminations. Next, we focus on the reconstruction of the sparse radar scene using the improved StOMP algorithm.

A great deal of compressed sensing based methods have been applied to radar systems [9], [10], [11], [12], [13], which recover the target scene from fewer measurements than traditional methods. In [9], it is demonstrated that the compressed sensing can eliminate the need for matched filter at the receiver and has the potential to reduce the required sampling rate. In the context of Ground Penetrating Radar (GPR), [10] presents a compressed sensing based data acquisition and imaging algorithm. By exploiting the sparsity of targets in the spatial space, the proposed algorithm can generate sharper target space images with fewer measurements than the standard back projection methods. Recently, [12], [13] introduced additional sensing matrix H and compressed the received signal further by making nonadaptive, linear projections of the direct data sampled at the Nyquist frequency. In [12], the transmitted waveform is optimized to reduce the mutual coherence between the sensing matrix and the basis matrix, while in [13], the methods for optimizing the transmitted waveform and sensing matrix separately and simultaneously are both presented to decrease the cross correlations between different target responses. However, neither of these methods mention the hardware implementation of the additional sensing

matrix, which is very complex and expensive.

In this paper, we are considering to reconstruct the sparse signal representing the radar scene directly based on the basis dictionary which is comprised of spatial-time steering vectors. This requires neither optimizing the transmission waveform nor changing the existing hardware system. However, the basis dictionary is with high coherence, which can not guarantee a perfect reconstruction with large probability. An improved StOMP algorithm is proposed to select multiple atoms to encapsulate the highly coherent columns (atoms) with high residual correlations at each iteration. This method can cope with the highly coherent columns efficiently. The proposed method uses a set of mixture Gaussian models to approximate the distribution of the residual correlations, and selects the coordinates among the top $t\%$ of each mixture Gaussian model.

The main contribution of the paper has three components: First, we present a novel CS-TBD algorithm, which avoids the nonlinear problem encountered in the traditional TBD algorithms. Secondly, an improved StOMP algorithm is proposed to reconstruct the whole radar scenario (DOA-Doppler plane) for each range gate at consecutive scans using the spatial-time data. Thirdly, in the proposed CS-TBD algorithm, the improved StOMP algorithm together with the temporal tracking performed during each scan effectively distinguishes true targets from false targets and clutters based on the information from multiple illuminations.

The paper is organized as follows: Section II introduces a discrete-time signal model for a typical space-time scenario in a TBD framework. The improved StOMP algorithm is introduced in Section III, and the CS-TBD algorithm is introduced in Section IV. The simulation results are listed in Section V, and the paper is summarized in Section VI.

II. A General Space Time Model and Its Sparse Representation

This section introduces a discrete-time signal model for a typical spacial-time scenario in a TBD framework. Without loss of generality, let us consider a radar system equipped with a uniform linear array of N identical sensors with inter-element spacing d. The steered array scans the surveillance area M times before deciding whether or not a target is present. During the m^{th} scan the following train of K pulses is transmitted [3]

$$\Re e\{Ae^{j\varphi}\sum_{k=1}^{K}p(t-(k-1)T-(m-1)\Delta)e^{j2\pi f_c t}\}, \quad t\in[(m-1)\Delta,(m-1)\Delta+KT], \tag{1}$$

where $\Re e\{z\}$ indicates the real part of the complex number z, and $A>0$ is an amplitude factor related to the transmitted power. $\varphi\in[0,2\pi)$ is the initial phase of the carrier signal. $p(t)$ is a unit-energy rectangular pulse waveform of duration T_p and one-sided bandwidth $W_p\approx 1/T_p$. T is the pulse repetition time, and $\Delta\geq KT$ is the scan repetition time. $f_c=c/\lambda$ is the carrier frequency, where c and λ denote the velocity of propagation in the medium and the carrier wavelength respectively.

We assume that Q point-like and slowly fluctuating targets are moving within the surveillance area and in the array far field. The radial velocity of the q^{th} target in the m^{th} scan is v_m^q. Neglecting compression or stretching of the time scale, the complex envelope of the received signal at the i^{th} sensor and over the m^{th} scan is given by [3],

$$\begin{aligned} r_m^i(t) &= \sum_{q=1}^{Q}\{\alpha_m^q e^{j2\pi(i-1)\nu_{sm}^q}e^{j2\pi f_m^q\cdot t}\cdot \\ &\quad \sum_{k=1}^{K}p(t-(k-1)T-(m-1)\Delta-\tau_m^q)\}+w_m^i(t), \\ &\quad i=1,\cdots,N,\ m=1,\cdots,M, \end{aligned} \tag{2}$$

where $\alpha_m^q\in C$ is a factor which accounts for $Ae^{j\varphi}$, the effects of the transmitting antenna gain, the radiation pattern of the array sensors, the two-way path loss, the radar cross section of the q^{th} target, etc. τ_m^q is the round-trip delay of the received signal for the q^{th} target (with respect to the origin of the reference system). f_m^q is the Doppler frequency shift of the signal backscattered by the q^{th} target (i.e., $f_m^q=(2v_m^q/c)f_c$). ν_{sm}^q is the q^{th} target's spatial frequency, i.e.,

$$\nu_{sm}^q=(d/\lambda)\sin(\theta_m^q), \tag{3}$$

with θ_m^q the DOA angle of the q^{th} target. $w_m^i(t)$ is the complex envelope of the overall disturbance.

In order to generate the vector of the noisy returns corresponding to the l^{th} range gate, $l=1,\cdots,L$, the received signal $r_m^i(t)$ is sampled at

$$t_{l,m,k}=t_{min}+(l-1)T_p+(k-1)T+(m-1)\Delta, \quad k=1,\cdots,K, \tag{4}$$

and the time samples are grouped to form an NK-dimensional vector as follows,

$$\begin{aligned} & z_{l,m} \\ = \ & vec\begin{bmatrix} r_m^1(t_{l,m,1}) & r_m^1(t_{l,m,2}) & \cdots r_m^1(t_{l,m,K}) \\ r_m^2(t_{l,m,1}) & r_m^2(t_{l,m,2}) & \cdots r_m^2(t_{l,m,K}) \\ \cdots & \cdots & \cdots \\ r_m^N(t_{l,m,1}) & r_m^N(t_{l,m,2}) & \cdots r_m^N(t_{l,m,K}) \end{bmatrix} \\ = \ & s_{l,m}+n_{l,m}, \end{aligned} \tag{5}$$

where vec is the vec operator [3], $s_{l,m}$ and $n_{l,m}$ denote the signal component and the noise component respectively.

Let t_{min} denote the beginning of the sampling process. Then the round-trip delay ς_m^l of the received signal at the l^{th} range gate of the m^{th} scan is given by

$$\varsigma_m^l=t_{min}+(l-1)T_p, \quad \varsigma_m^l\in[t_{min},t_{min}+(L-1)T_p]. \tag{6}$$

Hence, $z_{l,m}$ can be written as,

$$z_{l,m}=\begin{cases} \sum_{q=1}^{B_m^l}\alpha_m^{q,l}p(\varsigma_m^l)(S_{T,m}^{q,l}\otimes S_{S,m}^{q,l})+n_{l,m}, & B_m^l>0, \\ n_{l,m}, & B_m^l=0, \end{cases} \tag{7}$$

where B_m^l is the number of targets contained in the data from the l^{th} range gate of the m^{th} scan, and $B_m^l = 0$ indicates that there are no targets at the l^{th} range gate. We have $p(\varsigma_m^l) = 1$ considering that $p(t)$ is a unit-energy rectangular pulse waveform, and (7) can be further reduced to

$$z_{l,m} = \begin{cases} \sum_{q=1}^{B_m^l} \alpha_m^{q,l}(S_{T,m}^{q,l} \otimes S_{S,m}^{q,l}) + n_{l,m}, & B_m^l > 0, \\ n_{l,m}, & B_m^l = 0, \end{cases} \tag{8}$$

where $S_{S,m}^{q,l}$ and $S_{T,m}^{q,l}$ denote the spatial steering vector and the Doppler filtering steering vector for the q^{th} target at the l^{th} range gate respectively, and '$\otimes$' represents the Kronecker product of two vectors. The spatial steering vector $S_{S,m}^{q,l}$ and the Doppler filtering steering vector $S_{T,m}^{q,l}$ can be represented by

$$S_{S,m}^{q,l} = [1, e^{j\frac{2\pi d}{\lambda}\sin\theta_m^{q,l}}, \cdots, e^{j(N-1)\frac{2\pi d}{\lambda}\sin\theta_m^{q,l}}]^T \tag{9}$$

and,

$$S_{T,m}^{q,l} = [1, e^{j2\pi f_m^{q,l}\cdot T}, \cdots, e^{j(K-1)2\pi f_m^{q,l}\cdot T}]^T. \tag{10}$$

In this paper, the compressed sensing is used to reconstruct a DOA-Doppler plane based on $z_{l,m}$, the data from the l^{th} range gate at the m^{th} scan. In practice, the radar system has no knowledge of the number and locations of the targets. To do so, the DOA-Doppler plane is divided into $V \times D$ grids, where V and D denote the number of rows (for DOA angle) and columns (for Doppler frequency), respectively. Each grid is with the same size $\Delta\theta \times \Delta f$. The intersection of the i^{th} DOA angle bin and the j^{th} Doppler frequency bin represents a unique point (θ_i, f_j) with a corresponding reflection coefficient $\alpha(\theta_i, f_j)$. All the intersection points in the DOA-Doppler plane are mapped into a $VD \times 1$ vector x with the j^{th} column placed at the end of the $(j-1)^{th}$ column. As a result, the $((i-1)\cdot D+j)^{th}$ element of x corresponds to point (θ_i, f_j), which is defined as: $x((i-1)\cdot D+j) = \alpha(\theta_i, f_j)$.

Based on the above derivation, the measurement data $z_{l,m}$ can be represented in a compressed sensing framework as in (11),

$$z_{l,m} = \Phi x_{l,m} + n_{l,m}, \tag{11}$$

where $x_{l,m}$ is defined above. Φ is an $NK \times VD$ basis dictionary as $\Phi = [\varphi_1 \ \varphi_2 \ \cdots \ \varphi_{VD}]$ in columns. The $((i-1)\cdot D + j)^{th}$ column of Φ, which corresponds to the $((i-1)\cdot D + j)^{th}$ element of $x_{l,m}$, is defined as follows,

$$\varphi_{(i-1)\cdot D+j} = S_T(f_j) \otimes S_S(\theta_i). \tag{12}$$

Equation (11) constitutes the foundation of our proposed method. Without loss of generality, the radar scene is assumed to be sparse, resulting in a sparse vector $x_{l,m}$. Given $z_{l,m}$ and measurement noise $n_{l,m}$, the sparse vector $x_{l,m}$ can be reconstructed using a compressed sensing based method. For simplicity, (11) is rewritten as a standard model in compressed sensing,

$$y = \Phi x + e, \tag{13}$$

where y, x and e denote the measurement vector, the original sparse vector and the noise vector respectively.

III. Improved StOMP Algorithm

In this paper, we are considering to reconstruct the sparse signal representing the radar scene directly based on the basis dictionary which is comprised of spatial-time steering vectors. However, the basis dictionary built in TBD (12) is with high coherence, which can not guarantee a perfect reconstruction with large probability. An improved StOMP algorithm is proposed to select multiple atoms to encapsulate the highly coherent columns (atoms) with high residual correlations at each iteration. This method can cope with the highly coherent columns efficiently.

The steps of the proposed algorithm are same with those of the StOMP algorithm except the thresholding step. In the StOMP algorithm, the thresholds are specially chosen based on the assumption of Gaussianity of the residual correlations. Thresholding yields a small set of large coordinates which are beyond a formal noise level. However, the basis dictionary built in TBD (12) is a highly coherent matrix and the residual correlations do not satisfy the Gaussianity any more. In the proposed method, a set of mixture Gaussian models are used to approximate the distribution of the residual correlations. The proposed algorithm selects the coordinates among the top $t\%$ of each mixture Gaussian model. The detailed procedure of the proposed algorithm is listed in the following.

Algorithm 1: Improved StOMP Algorithm:
INPUT: Measurement vector y
OUTPUT: Index set I, reconstructed vector $\hat{v} = x$
(1): Initialize: Let the index set $I = \emptyset$ and the residual $r = y$. Repeat the following steps times or until $r = 0$:
(2):Threshold: Apply matched filtering to the current residual as

$$u = \Phi^* r, \tag{14}$$

where u is a vector of residual correlations. A set of mixture Gaussian models is then used to approximate the distribution of the residual correlations. For each mixture Gaussian model, choose the coordinates among the top $t\%$ of it. All the obtained coordinates form a set J.
(3): Update: Add the set J to the index set: $I \longleftarrow I \cup J$, and update the residual

$$x = \underset{\hat{v}\in\Re^I}{argmin}\, ||z - \Phi\hat{v}||_2; \qquad r = z - \Phi x. \tag{15}$$

However, with small probability, some additional entries (false targets) occur in the reconstructed sparse vector due to the highly coherent columns. Fortunately, the temporal tracking performed during each scan can effectively identify the true targets from the false targets based on the information from multiple illuminations.

IV. The Proposed CS-TBD Algorithm

This section introduces the CS-TBD algorithm, which is mainly divided into two steps. First, the proposed algorithm

reconstructs the whole radar scenario (direction of arrival (DOA)-Doppler plane) using an improved StOMP algorithm, which has been introduced in Sections II and III. The proposed algorithm then performs temporal tracking in the newly built three-dimensional range-DOA-Doppler space.

Since the width of the antenna beam is finite, a target is usually hit by a set of successive illuminations during each scan [1]. Thus in this paper, temporal tracking is performed inside each scan (in the three dimensional space comprised of range, DOA and Doppler), as well as among consecutive scans. As a result, the temporal tracking (TBD) consists of two main procedures: the TBD performed inside one scan, and the TBD performed among consecutive scans.

First, the TBD performed inside one scan is considered. For the l^{th} range gate at the m^{th} scan, we can reconstruct the sparse signal $x_{l,m}$ using the improved StOMP algorithm, based on which a radar scenario (DOA-Doppler plane) is built. The $((i-1)\cdot D+j)^{th}$ element of $x_{l,m}$ corresponds to the point (θ_i, f_j) in the reconstructed DOA-Doppler plane. As a result, L DOA-Doppler planes are built in the m^{th} scan, resulting in a three-dimensional DOA-Doppler-range space. The intersection of the i^{th} DOA angle bin and the j^{th} Doppler frequency bin in the l^{th} range gate plane represents a unique point (θ_i, f_j, l). A simple procedure is then used to distinguish the points occupied by the potential targets from the points corresponding to noise (Algorithm 2). The potential targets are with large reflection coefficients.

Algorithm 2: Let $PT_{l,m}(c)$ denote the c^{th} potential target at the l^{th} range gate at the m^{th} scan and set $c=0$. For $l=1,\cdots,L$,

(1): $x_{l,m}=Reconstruct(\Phi, z_{l,m})$;

(2): For $i=1,\cdots,VD$,

if $|x_{l,m}(i)|>T_{target}$

$x_{l,m}(i)$ corresponds to a potential target,

$c=c+1$,

$PT_{l,m}(c)=x_{l,m}(i)$,

else

$x_{l,m}(i)$ corresponds to noise and is set as zero.

end

Here '$Reconstruct$' refers to the improved StOMP algorithm. T_{target} is a threshold set to distinguish the potential targets from noise. It should be noted that the potential targets consist of the true targets, false targets and clutter. The false targets are wrongly generated by the improved StOMP algorithm due to the highly coherent columns.

A K-means method is then utilized to cluster the points (potential targets) obtained from Algorithm 2 in the three-dimensional DOA-Doppler-range space at the m^{th} scan, based on which a track is formed for each potential target. It is assumed that the true target is hit by more than NL consecutive illuminations in each scan. Therefore, a track consisting of NL points would correspond to a true target, while the track consisting of less than NL points would correspond to a false target or clutter, and be removed. The reason is that compared with the true target which moves continuously in the three-dimensional space according to a general dynamic model, the false target appears randomly in the three-dimensional space. Furthermore, considering that the DOA angle and velocity of a target keep invariant during one scan, a simpler projection method is adopted to distinguish the true targets from the false targets and clutter in the simulation example (refer to Section V).

Next, we consider the TBD process performed among consecutive scans. From the above derivation, we can obtain a three-dimensional space for each scan. A series of three-dimensional spaces corresponding to M consecutive scans are combined to one final three-dimensional space, and the tracks corresponding to one specific target in different scans would connect to each other in the final three-dimensional space. This results in a number of final tracks consisting of multiple scan information, each for a true target.

Complexity Analysis Here we will analyze the computational complexity of the proposed CS-TBD algorithm, and further make a comparison to the traditional TBD algorithm [3] on computational complexity.

The CS-TBD algorithm consists of two steps. First, the proposed algorithm reconstructs the DOA-Doppler plane for each range gate at consecutive scans using an improved StOMP algorithm. The proposed algorithm then performs temporal tracking in the newly built three-dimensional range-DOA-Doppler space. The computational complexity mainly focuses on the reconstruction of the radar scenario for each range gate at consecutive scans using an improved StOMP algorithm. The cost of reconstruction work is of the order of $O(ML\cdot O(StOMP))$, where O denotes order. M is the total number of scans that are jointly processed in the TBD framework, and L is the number of illuminations in each scan. $O(StOMP)=\eta(\mu+2)N_1N_2+O(N_2)$ indicates the complexity of the StOMP algorithm according to [8]. N_1 and N_2 denote the number of rows and columns of the sensing matrix respectively. μ and η denote the total number of conjugate gradient iterations and StOMP stages respectively, and both are small constants.

The process of complexity analysis of the traditional TBD is similar to that of [1]. The total cost of the traditional TBD is of the order of $O(MLN_cN_\phi)$, where N_ϕ and N_c are respectively the number of azimuthal radar sectors and the number of non-ambiguous range gates in a scan.

From the above deviations, we have that the computational complexity of the proposed CS-TBD algorithm is of the order of $O(ML\cdot O(StOMP))\approx O(MLN_1N_2)$ considering that μ and η are small constants, which is comparable to that of the traditional TBD algorithm if N_1N_2 and N_cN_ϕ are with the same orders.

V. Simulation Results and Analysis

The simulation example considers two perspective targets approaching the radar, one is with a relative radial velocity of $100m/s$ and a DOA angle of 10 degree, beginning from the range gate which is $2000m$ away from the position of the radar. The other is with a relative radial velocity of

TABLE I
SIMULATION PARAMETERS

Simulation Parameter	Value
Pulse shape	Rectangular
Carrier frequency	10 GHz
T_p	$0.5\ \mu s$
PRF	$820\ Hz$
T_R	$2.09s$
Number of sensors (N)	5
Number of pulses (K)	5
Number of rows of DOA-Doppler plane (V)	20
Number of columns of DOA-Doppler plane (D)	30
Threshold T_{target}	0.5
NL	4

$150m/s$ and a DOA angle of 20 degree, beginning from the same range gate as the first one. The range of the DOA angle and Doppler frequency are $[0^o, 30^o]$, and $[0Hz, 4000Hz]$ respectively. The clutter is assumed uniformly distributed with density $1 \times 10^{-6}/m^2$. The scan interval is $1s$ with totally ten illuminations. More simulation parameter are listed in Table I.

The simulation results obtained from inside one scan are shown in Figs $1 \sim 2$. Fig. 1 shows that the reconstructed potential targets are comprised of the estimates of true targets (the stars inside the red circles), the estimates of clutter (the stars inside the triangles), and the estimates of false targets due to the highly coherent columns (the independent stars). Moreover, it can be seen that both of the two targets are lost in tracking at range gate 2000. Next, we are going to distinguish the estimates of true targets from the estimates of false targets and clutter. It is reasonable to assume that the DOA angle and velocity of a target keep invariant during one scan. All the points are then projected to a DOA-Doppler plane and clustered (Fig. 2). The resulting two clusters locate around $(10^o, 2000Hz)$ and $(20^o, 3000Hz)$ respectively. Each cluster consists of more than NL points and corresponds to a true target.

The simulation results obtained from five consecutive scans are shown in Fig. 3. A series of three-dimensional spaces corresponding to five consecutive scans are combined to one final three-dimensional space, and the tracks corresponding to one specific target in different scans would connect to each other in the final three-dimensional space (Fig. 3). This results in two final tracks consisting of multiple scan information, each for a true target.

VI. CONCLUSION

A novel CS-TBD algorithm is proposed in this work. Different from the existing TBD algorithms that adopt hypothesis test using the radar measurement, the proposed algorithm reconstructs the whole radar scenario (DOA-Doppler plane) for each range gate at consecutive scans using an improved StOMP algorithm. Temporal tracking is performed inside each scan (in the three dimensional space comprised of range, DOA and Doppler), as well as among consecutive scans. The simulation results show that the proposed algorithm can track and detect multiple targets successfully.

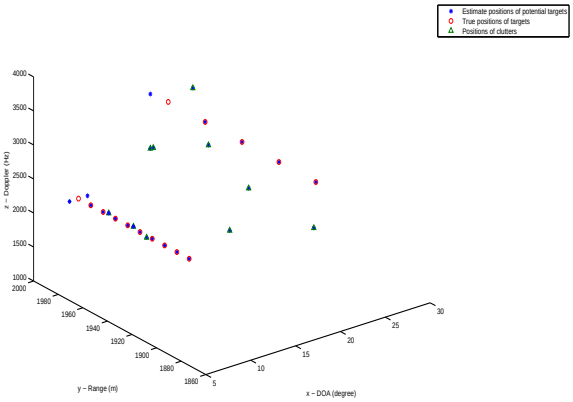

Fig. 1. Original Reconstructed Radar Scene

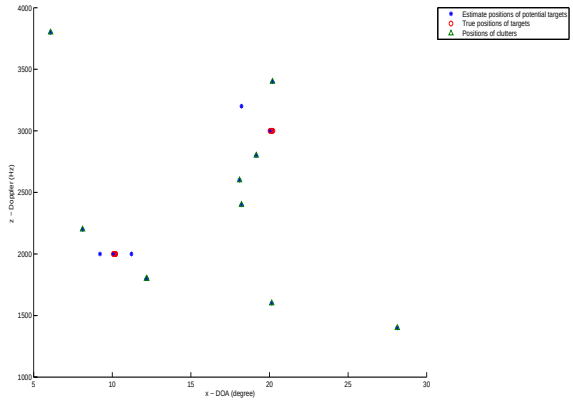

Fig. 2. Projected Reconstructed Radar Scene

ACKNOWLEDGMENT

This work was supported by the Natural Science Foundations of China (No. 61104051, No.61074176 and No.61004087), the Fundamental Research Funds for the Central Universities, and the Scientific Research Foundation for the Returned Overseas Chinese Scholars, State Education Ministry.

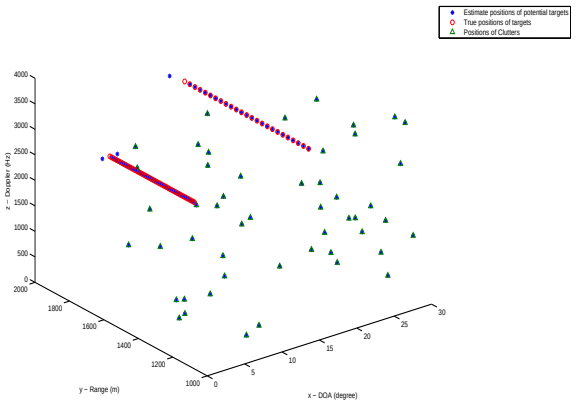

Fig. 3. TBD among consecutive scans

REFERENCES

[1] S. Buzzi, M. Lops, and L. Venturino, "Track-before-detect procedures for early detection of moving target from airborne radars," *IEEE Transaction on Aerospace and Electronic Systems*, vol. 41, no. 3, pp. 937–954, Jul. 2005.

[2] D. Orlando, L. Venturino, M. Lops, and G. Ricci, "Track-before-detect strategies for stap radars," *IEEE Transactions on Signal Processing*, vol. 58, no. 2, pp. 933–938, Feb. 2010.

[3] D. ORLANDO, G. RICCI, and Y. BAR-SHALOM, "Track-before-detect algorithms for targets with kinematic constraints," *IEEE Transaction on Aerospace and Electronic Systems*, vol. 47, no. 3, pp. 1837–1849, Jul. 2011.

[4] B. Ristic, S. Arulampalam, and N. J. Gordon, *Beyond the Kalman Filter: Particle Filters for Tracking Applications*. Norwood, MA: Artech House, 2004.

[5] H. Im and T. Kim, "Optimization of multiframe target detection schemes," *IEEE Transaction on Aerospace and Electronic Systems*, vol. 35, no. 1, pp. 176–186, Jan. 1999.

[6] L. A. Johnston and V. Krishnamurthy, "Performance analysis of a dynamic programming track before detect algorithm," *IEEE Transaction on Aerospace and Electronic Systems*, vol. 38, no. 1, pp. 228–242, Jan. 2002.

[7] J. Liu, C. Han, X. Yao, and F. Lian, "Compressed sensing based track before detect algorithm for airborne radars," *Progress In Electromagnetics Research*, vol. 138, pp. 433–451, 2013.

[8] D. L. Donoho, Y. Tsaig, I. Drori, and J. C. Starck, "Sparse solution of underdetermined linear equations by stagewise orthogonal matching pursuit," *IEEE TRANSACTIONS ON INFORMATION THEORY*, vol. 58, no. 2, pp. 1094–1121, Feb. 2012.

[9] R. Baraniuk and P. Steeghs, "Compressive radar imaging," in *Proc. Radar Conference*, April 2007, pp. 128–133.

[10] A. Gurbuz, J. McClellan, and W. Scott, "Compressive sensing for GPR imaging," in *Proc. 41th Asilomar Conf. Signals, Syst. Comput*, Nov. 2007, pp. 2223–2227.

[11] J. H. Ender, "On compressive sensing applied to radar," *Signal Processing*, vol. 90, pp. 1402–1414, 2010.

[12] Y. Yu, A. Petropulu, and H. Poor, "Measurement matrix design for compressive sensingcbased MIMO radar," *IEEE Transactions on Signal Processing*, vol. 59, no. 11, pp. 5338–5352, 2011.

[13] J. Zhang, D. Zhu, and G. Zhang, "Adaptive compressed sensing radar oriented toward cognitive detection in dynamic sparse target scene," *IEEE Transactions on Signal Processing*, vol. 60, no. 4, pp. 1718–1729, Apr. 2012.